Journal of Peptide Science
J. Peptide Sci. **10**: 510–523 (2004)
Published online 2 February 2004 in Wiley InterScience (www.interscience.wiley.com). DOI: 10.1002/psc.562

JOURNAL OF PEPTIDE SCIENCE

Hybrid α/β^3-Peptides with Proteinogenic Side Chains. Monosubstituted Analogues of the Chemotactic Tripeptide For-Met-Leu-Phe-OMe

CESARE GIORDANO,[a] GINO LUCENTE,[a]* ADRIANO MOLLICA,[a] MARIANNA NALLI,[a] GIAMPIERO PAGANI ZECCHINI,[a] MARIO PAGLIALUNGA PARADISI,[a] ENRICO GAVUZZO,[b] FERNANDO MAZZA[c] and SUSANNA SPISANI[d]

[a] Istituto di Chimica Biomolecolare, CNR, and Dipartimento di Studi Farmaceutici, Università di Roma 'La Sapienza', 00185 Roma, Italy
[b] Istituto di Cristallografia, CNR, CP 10, 00016 Monterotondo Stazione, Roma, Italy
[c] Dipartimento di Chimica, Ingegneria Chimica e Materiali, Università di L' Aquila, 67010 Coppito, L' Aquila, Italy
[d] Dipartimento di Biochimica e Biologia Molecolare, Università degli Studi di Ferrara, 44100 Ferrara, Italy

Received 29 October 2003
Accepted 2 December 2003

Abstract: The α/β^3-mixed tripeptides R-CO-β^3-HMet-Leu-Phe-OMe (**1a**,**b**), R-CO-Met-β^3-HLeu-Phe-OMe (**2a**,**b**) and R-CO-Met-Leu-β^3-HPhe-OMe (**3a**,**b**) (**a**, R = *tert*-butyloxy-; **b**, R = H-), analogues of the potent chemoattractant For-Met-Leu-Phe-OMe, have been synthesized by classical solution methods and fully characterized. The activities of the new analogues as chemoattractants, superoxide anion producers and lysozyme releasers have been determined on human neutrophils. Whereas all of the three *N*-formyl derivatives are significantly less active than the parent tripeptide as chemoattractants, compound **1b** has been found to be highly active as a superoxide anion producer and **3b** as a lysozyme releaser. The results show that the replacement of the native Leu residue at the central position is, in each of the examined cases, the least favourable modification. The three *N*-Boc derivatives are, as expected, devoid of activity as agonists, but they are all good inhibitors of chemotaxis. Information on the solution conformation has been obtained by examining the involvement of the NH groups in intramolecular H-bonds using ^{1}H NMR. The conformation of the *N*-Boc analogue **1a** has also been determined in the crystal state by x-ray diffraction analysis. The molecule is extended at the β^3-HMet residue ($\varphi_1 = -87°$; $\theta_1 = 172°$; $\psi_1 = 126°$) and no intramolecular H-bond is present.

Keywords: β-amino acids; chemotactic peptides; crystal structure; peptide conformation; β-peptides

Abbreviations: Amp, 2-amino-1-phenylpropane; Boc, *tert*-butyloxycarbonyl; DMF, *N,N*-dimethylformamide; DMSO, dimethylsulphoxide; EEDQ, ethyl 2-ethoxy-1,2-dihydro-1-quinolinecarboxylate; EtOAc, ethyl acetate; β^3-HLeu, L-β^3-homoleucine (S isomer); β^3-HMet, L-β^3-homomethionine (*R* isomer); β^3-HPhe, L-β^3-homophenylalanine (S isomer); KRPG, Krebs-Ringer-phosphate containing 0.1% w/v D-glucose (pH 7.4); NMM, *N*-methylmorpholine; O*i*-Bu, *iso*-butyloxy; OMe, methoxy.

* Correspondence to: Gino Lucente, Dipartimento di Studi Farmaceutici, Università di Roma 'La Sapienza', P.le A. Moro, 5, 00185 Roma, Italy; e-mail: gino.lucente@uniroma1.it

INTRODUCTION

The chemotactic *N*-formylpeptides are involved in defence mechanisms against bacterial infections through binding with specific receptors located on neutrophil membranes [1]. The *N*-formyl tripeptide methyl ester *N*-For-Met-Leu-Phe-OMe (fMLF-OMe) represents the reference molecular model for *N*-formylpeptide receptor ligands and is the most extensively studied member of this group of bioactive peptides [2]. In addition to chemotaxis (cell migration towards an increasing concentration of the stimulus), *N*-formylpeptides can also stimulate different biochemical events among which are activation of superoxide anion production and release of lysosomal enzymes [3].

During our research on the structure–activity relationships in the field of chemotactic peptides related to fMLF-OMe a programme was started recently centred on the examination of the biochemical consequences of introducing achiral, ω-amino acid residues, including β-Ala (β-HGly), at the central position of the reference ligand fMLF-OMe [4,5]. As a continuation of this research and taking into account the increasing interest in peptidomimetics obtained by replacing the native α-residues with β-amino acids bearing a proteinogenic side chain [for leading review articles see references 6–9], this report examines three α/β^3-mixed peptide analogues of fMLF-OMe. In particular, the synthesis, biological activities and conformational properties in solution of the following compounds are reported: [β^3-HMet^1]fMLF-OMe (**1b**), [β^3-HLeu^2]fMLF-OMe (**2b**) and [β^3-HPhe^3]fMLF-OMe (**3b**) (Figure 1). The corresponding *N*-Boc derivatives **1a**–**3a**, obtained as intermediates during the synthesis of the above mentioned *N*-For peptides, have been also examined for their activity as chemotactic antagonists. The conformation adopted in the crystal state by the β^3-HMet^1 containing analogue Boc-β^3-HMet-Leu-Phe-OMe (**1a**) is also reported. It should be noted here that, although peptides solely composed by β-amino acids (β-peptides) are extensively studied and their propensity to adopt well defined secondary structures is well established [6–9], the heterooligomers made up of both α- and β-amino acids have received considerably less attention [10–17]. These latter compounds possess, however, a significant potential in the design of bioactive peptidomimetics. This property is essentially due to their propensity to adopt characteristic secondary structures even in short oligomers and to their enhanced stability towards mammalian peptidases [18–20]. Although chemotactic *N*-formylpeptides containing the achiral β-Ala residue have been previously described [5,21], the compounds reported here represent, to the best of our knowledge, the first fMLF-OMe analogues obtained by following the α/β^3-peptide approach.

EXPERIMENTAL

Peptide Synthesis and Characterization

General. Melting points were determined with a Kofler hot-stage apparatus and are uncorrected. Optical rotations were taken at 20 °C with a Schmidt–Haensch Polartronic D polarimeter (1 dm cell, *c* 1.0 in $CHCl_3$). IR absorption spectra (KBr disks) were recorded employing a Perkin-Elmer FT-IR Spectrum 1000 spectrometer.

^{1}H NMR spectra were determined in $CDCl_3$ solution with a Bruker Avance 400 spectrometer using Me_4Si as the internal standard. Column chromatographies were carried out using Merck silica gel 60 (230–400 mesh). Thin-layer and preparative layer chromatographies were performed on Merck 60 F_{254} silica gel plates. Light petroleum refers to the 40°–60 °C b.p. fraction. The drying agent was sodium sulphate. Boc-protected β^3- and α-amino acids were purchased from Fluka, Switzerland and fMLF-OMe from Sigma, USA. Boc-β-Ala-Phe-OMe (**4a**) was synthesized as previously reported [5]. The synthesis of the *N*-protected, α/β^3-mixed tripeptides **1**–**3** and related dipeptide models was performed in solution by adopting conventional procedures. The strategies and details of the reagents are reported in Figure 1.

HCl·H-β^3-HPhe-OMe. Thionyl chloride (0.076 ml, 1.05 mmol) was added to a solution of Boc-β^3-HPhe-OH (0.279 g, 1 mmol) in dry methanol (1 ml), cooled at −15 °C. After stirring at −15 °C for 30 min and at 45 °C for 2.5 h, the solution was evaporated *in vacuo* to give the pure amino ester hydrochloride in quantitative yield. Melting point, optical rotation, IR absorption and NMR data are in accord with those previously reported for the *R* isomer [22].

General procedure for the synthesis of Boc-α/β^3-mixed dipeptides. Isobutyl chloroformate (0.13 ml, 1 mmol) and NMM (0.132 ml, 1.2 mmol) were added at −15 °C to a stirred solution of Boc-β^3-HLeu-OH (1 mmol) in the case of Boc-β^3-HLeu-Phe-OMe or

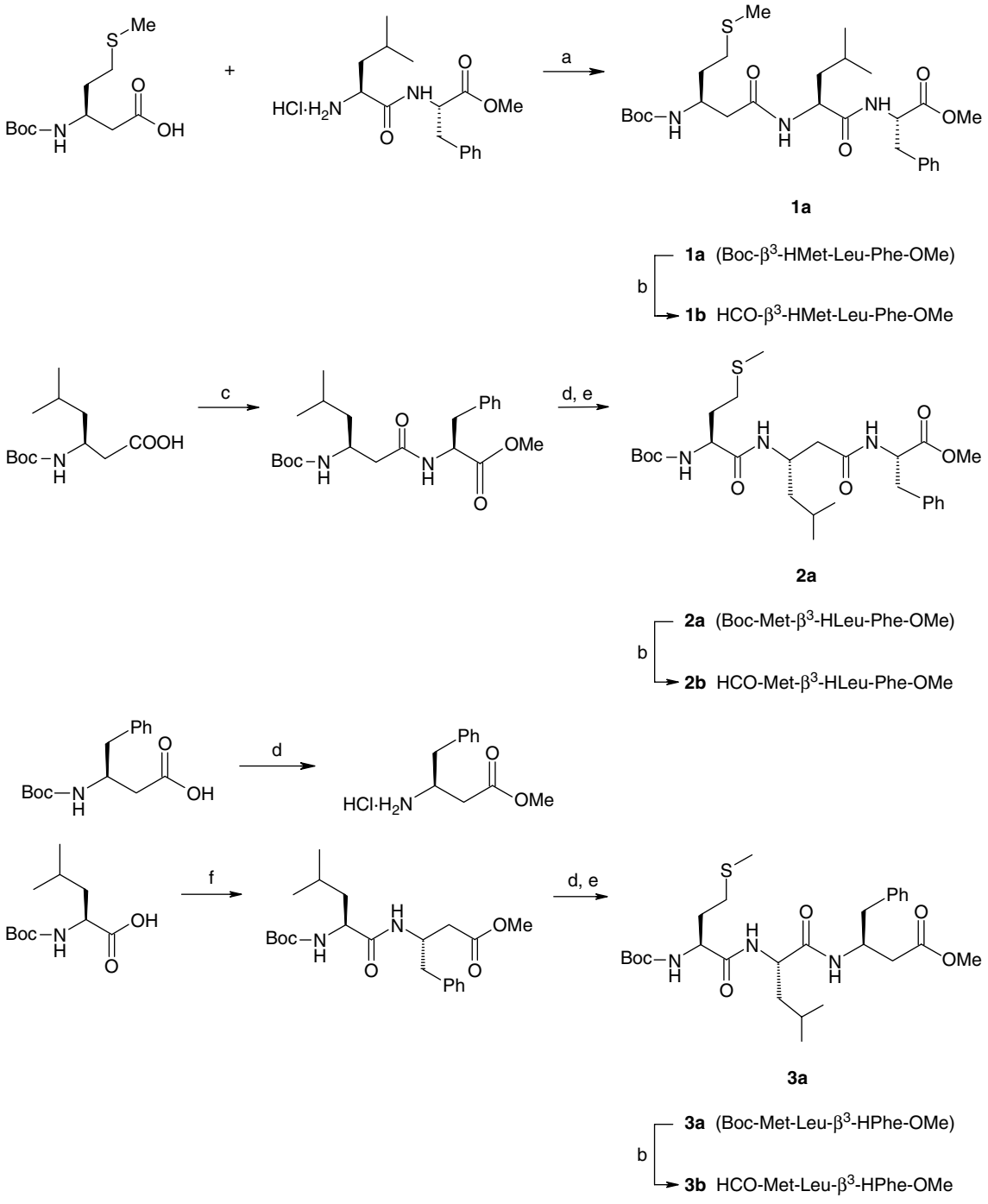

Figure 1 Methods of synthesis for the *N*-protected mixed tripeptides **1**–**3**. a: *i*-BuOCOCl, NMM; b: HCOOH, EEDQ; c: *i*-BuOCOCl, NMM, HCl·H-Phe-OMe; d: $SOCl_2$, MeOH; e: Boc-Met-OH, *i*-BuOCOCl, NMM; f: i-BuOCOCl, NMM, HCl·H-β^3-HPhe-OMe.

of Boc-Leu-OH (1 mmol) in the case of Boc-Leu-β^3-HPhe-OMe in dry CH_2Cl_2 (5 ml). The temperature was maintained at −15 °C for 10 min, and HCl·H-Phe-OMe (1 mmol) or HCl·H-β^3-HPhe-OMe (1 mmol), NMM (0.11 ml, 1 mmol) and dry CH_2Cl_2 (3.6 ml) were added. The mixture was stirred at −15 °C for 15 min and then allowed to warm to room temperature. Dry DMF (10 drops) was added and

stirring was continued for 1 day. EtOAc was added in excess and the organic layer washed with 2N HCl, brine, saturated aqueous $NaHCO_3$ and brine. The organic phase was dried and evaporated to give pure solid dipeptides in quantitative yields.

Boc-β³-HLeu-Phe-OMe. m.p. 150.5°–151 °C (EtOAc); $[\alpha]_D$ + 21°; IR ν_{max} 3353, 1752, 1682, 1647, 1528 cm^{-1}; ^1H NMR δ 0.89 [6H, d, J = 6.5 Hz, $CH(CH_3)_2$], 1.20–1.72 [3H, m, $CH_2CH(CH_3)_2$], 1.44 [9H, s, $C(CH_3)_3$], 2.37 (2H, m, β^3-HLeu α-CH_2), 3.06 and 3.14 (2H, A and B of an ABX, J = 5.9, 6.5 and 13.9 Hz, Phe β-CH_2), 3.71 (3H, s, $COOCH_3$), 3.89 (1H, m, β^3-HLeu β-CH), 4.87 (1H, m, Phe α-CH), 4.97 (1H, br, β^3-HLeu NH), 6.17 (1H, poorly resolved d, Phe NH), 7.10–7.35 (5H, m, aromatic).

Boc-Leu-β³-HPhe-OMe. m.p. 114°–115 °C (EtOAc-*n*-hexane); $[\alpha]_D$ −47°; IR ν_{max} 3328, 3301, 1740, 1684, 1662, 1522 cm^{-1}; ^1H NMR δ 0.91 [6H, d, J = 6 Hz, $CH(CH_3)_2$], 1.35–1.70 [3H, m, $CH_2CH(CH_3)_2$], 1.44 [9H, s, $C(CH_3)_3$], 2.49 (2H, m, β^3-HPhe α-CH_2), 2.83 and 2.93 (2H, A and B of an ABX, J = 6.5, 8.0, 13.6 Hz, β^3-HPhe γ-CH_2), 3.68 (3H, s, $COOCH_3$), 4.03 (1H, m, Leu α-CH), 4.47 (1H, m, β^3-HPhe β-CH), 4.82 (1H, d, J = 6.7 Hz, Leu NH), 6.70 (1H, d, J = 8.7 Hz, β^3-HPhe NH), 7.14–7.33 (5H, m, aromatic).

General procedure for the synthesis of Boc-tripeptides 1a–3a. Thionyl chloride (0.076 ml, 1.05 mmol) was added to a solution of the above mentioned dipeptides (1 mmol) in dry methanol (1 ml), cooled at −15 °C. After stirring at −15 °C for 30 min and at 45 °C for 2.5 h, the solution was evaporated *in vacuo* to give the intermediate dipeptide ester hydrochlorides as foams. These salts were used without further purification. Boc-β^3-HMet-OH (1 mmol) in the case of **1a** and Boc-Met-OH (1 mmol) in the cases of **2a** and **3a** dissolved in dry CH_2Cl_2 (2.2 ml) were *C*-activated by adding isobutyl chloroformate (0.13 ml, 0.1 mmol) and NMM (0.132 ml, 1.2 mmol). Equivalent amounts of the dipeptide ester hydrochlorides or HCl·H-Leu-Phe-OMe and NMM were added in dry CH_2Cl_2 (1.6 ml) as described above for dipeptides. Usual work up afforded a pure material for **1a** and **3a**. Crude tripeptide **2a** (1 g) was purified by column chromatography using 40 g of silica gel ($CHCl_3$ as eluant).

1a. Yield: 99%; m.p. 160°–161 °C (EtOAc-light petroleum); $[\alpha]_D$ −7°; IR ν_{max} 3286, 1749, 1683, 1638, 1520 cm^{-1}; ^1H NMR δ 0.90 [6H, m, $CH(CH_3)_2$], 1.44 [9H, s, $C(CH_3)_3$], 1.48–2.00 [5H, m, β^3-HMet γ-CH_2 and $CH_2CH(CH_3)_2$], 2.09 [3H, s, SCH_3], 2.37–2.60 [4H, m, β^3-HMet α-CH_2 and δ-CH_2], 3.12 [2H, m, Phe β-CH_2], 3.73 [3H, s, $COOCH_3$], 3.91 [1H, m, β^3-HMet β-CH], 4.40 [1H, m, Leu α-CH], 4.61 [1H, m, Phe α-CH], 5.19 [1H, d, J = 8.2 Hz, β^3-HMet NH], 6.24 [1H, d, J = 7.9 Hz, Leu NH], 6.55 [1H, d, J = 7.7 Hz, Phe NH], 7.05–7.35 [5H, m, aromatic].

2a. Yield: 87%; m.p. 166.5°–168 °C (EtOAc); $[\alpha]_D$ + 11°; IR 3427, 1740, 1705, 1670 cm^{-1}; ^1H NMR δ 0.89 [6H, d, J = 6.3 Hz, $CH(CH_3)_2$], 1.23–1.62 [3H, m, $CH_2CH(CH_3)_2$], 1.43 [9H, s, $C(CH_3)_3$], 1.80–2.12 (2H, m, Met β-CH_2), 2.10 (3H, s, S-CH_3), 2.40 (2H, m, β^3-HLeu α-CH_2), 2.53 (2H, t, J = 7.3 Hz, Met γ-CH_2), 3.09 and 3.14 (2H, A and B of an ABX, J = 5.8, 6.4 and 14 Hz, Phe β-CH_2), 3.73 (3H, s, $COOCH_3$), 4.17 (2H, m, Met α-CH and β^3-HLeu β-CH), 4.84 (1H, m, Phe α-CH), 5.24 (1H, d, J = 7.8 Hz, Met NH), 6.20 (1H, d, J = 7.7 Hz, Phe NH), 6.81 (1H, d, J = 8.6 Hz β^3-HLeu NH), 7.10–7.35 (5H, m, aromatic).

3a. Yield: 97%; m.p. 114°–115 °C (EtOAc-*n*-hexane); $[\alpha]_D$ −55°; IR ν_{max} 3286, 1750, 1684, 1671, 1638, 1522 cm^{-1}; ^1H NMR δ 0.91 [6H, apparent t, $CH(CH_3)_2$], 1.43–1.70 [3H, m, $CH_2CH(CH_3)_2$], 1.46 [9H, s, $C(CH_3)_3$], 1.86–2.12 (2H, m, Met β-CH_2), 2.13 (3H, s, SCH_3), 2.45–2.63 (4H, Met γ-CH_2 and β^3-HPhe α-CH_2), 2.83 and 2.93 (2H, A and B of an ABX, J = 6.5, 8 and 13.6 Hz, β^3-HPhe γ-CH_2), 3.70 (3H, s, $COOCH_3$), 4.24 (1H, m, Met α-CH), 4.34 (1H, m, Leu α-CH), 4.47 (1H, m, β^3-HPhe β-CH), 5.17 (1H, d, J = 6.9 Hz, Met NH), 6.59 (1H, d, J = 7.9 Hz, Leu NH), 6.69 (1H, d, J = 7.9 Hz, β^3-HPhe NH), 7.16–7.35 (5H, m, aromatic).

General procedures for the synthesis of formyl-peptides 1b–4b. The Boc-peptides **1a**–**4a** (1 mmol) were dissolved in formic acid (6 ml) and the mixture stirred at room temperature for 1 day. After removal of the excess of formic acid *in vacuo*, the residue was dissolved in dry chloroform (6 ml) in the cases of **1b**, **3b** and **4b** or in dry DMF (6 ml) in the case of **2b**. EEDQ 97% (1.2 mmol) was added. The solution was stirred at room temperature for 24 h. Evaporation under reduced pressure afforded a solid residue in the case of **2b**, which was filtered and washed with dry diethyl ether. The foamy residues, obtained by evaporation of the reaction mixtures containing **1b**, **3b** and **4b**, were purified by preparative layer chromatography [$CHCl_3$–MeOH (95 : 5) as eluant].

1b. Yield: 70%; foam; $[\alpha]_D$ + 2°; IR ν_{max} 3288, 1748, 1654, 1630, 1542 cm^{-1}; ^1H NMR δ 0.90–0.93 [6H,

m, $CH(CH_3)_2$], 1.45–2.15 [5H, m, β^3-HMet γ-CH_2 and $CH_2CH(CH_3)_2$], 2.08 [3H, s, SCH_3], 2.47 [4H, br, m, β^3-HMet α-CH_2 and δ-CH_2], 3.12 [2H, m, Phe β-CH_2], 3.73 [3H, s, $COOCH_3$], 4.25–4.55 [2H, br, m, β^3-HMet β-CH and Leu α-CH], 4.52 [1H, m, Phe α-CH], 6.47 [1H, poorly resolved d, Leu NH], 6.55 [1H, d, $J = 8$ Hz, Phe NH], 6.77 [1H, poorly resolved d, β^3-HMet NH], 7.05–7.35 [5H, m, aromatic], 8.02 [1H, s, HCO].

2b. Yield: 93%; m.p. 182°–183 °C; $[\alpha]_D$ +16° ($c = 0.5$ in $CHCl_3$); IR ν_{max} 3303, 3085, 2966, 1752, 1651,1552 cm^{-1}; ^1H NMR δ 0.91 [6H, d, $J = 6.3$ Hz, $CH(CH_3)_2$], 1.30–1.55 [3H, two m, $CH_2CH(CH_3)_2$], 1.96–2.14 (2H, two m, Met β-CH_2), 2.13 (3H, s, SCH_3), 2.42 (2H, d, $J = 5.4$ Hz, β^3-HLeu α-CH_2), 2.56 (2H, m, Met γ-CH_2), 3.12 and 3.15 (2H, A and B of an ABX, $J = 5.8$, 6.3 and 14 Hz, Phe β-CH_2), 3.76 (3H, s, $COOCH_3$), 4.19 (1H, m, β^3-HLeu β-CH), 4.62 (1H, m, Met α-CH), 4.86 (1H, m, Phe α-CH), 6.10 (1H, d, $J = 7.7$ Hz, Phe NH), 6.51 (1H, d, $J = 7.5$ Hz, Met NH), 6.85 (1H, d, $J = 8.5$ Hz, β^3-HLeu NH), 7.10–7.35 (5H, m, aromatic), 8.22 (1H, s, HCO).

3b. Yield: 84%; foam; $[\alpha]_D$ −43°; IR ν_{max} 3276, 1710, 1689, 1638, 1554 cm^{-1}; ^1H NMR δ 0.92 and 0.91 [6H, two superimposed d, $J = 5.9$ Hz, $CH(CH_3)_2$], 1.45–1.68 [3H, m, $CH_2CH(CH_3)_2$], 1.94–2.10 (2H, m, Met β-CH_2), 2.12 (3H, s, SCH_3), 2.45–2.63 (4H, Met γ-CH_2 and β^3-HPhe α-CH_2), 2.83 and 2.93 (2H, A and B of an ABX, $J = 6.5$, 7.9 and 13.6 Hz, β^3-HPhe γ-CH_2), 3.70 (3H, s, $COOCH_3$), 4.41 (1H, m, Leu α-CH), 4.48 (1H, m, β^3-HPhe β-CH), 4.77 (1H, m, Met α-CH), 6.80 (1H, d, $J = 7.9$ Hz, Met NH), 6.87 (1H, d, $J = 8.7$ Hz, Phe NH), 6.93 (1H, d, $J = 7.9$ Hz, Leu NH), 7.15–7.35 (5H, m, aromatic), 8.21 (1H, s, HCO).

4b. Yield: 90%; m.p. 125°–127 °C (from EtOAc/*n*-hexane); $[\alpha]_D$+59°; IR ν_{max} ($CHCl_3$) 3428, 1742, 1682 cm^{-1}; ^1H NMR δ 2.37–2.41 (2H, m, β-Ala α-CH_2), 3.07 and 3.19 (2H, A and B of an ABX, $J = 5.6$, 6.7 and 13.9 Hz, Phe CH_2Ph), 3.47–3.55 (2H, m, β-Ala β-CH_2), 3.75 (3H, s, $COOCH_3$), 4.87 (1H, m, Phe α-CH), 5.92 (1H, d, $J = 7.4$ Hz, Phe NH), 6.19 (1H, m, β-Ala NH), 7.09–7.32 (5H, m, aromatic), 8.09 (1H, s, HCO).

Boc-β-Ala-Amp (5). Isobutyl chloroformate (0.13 ml, 1 mmol) was added at −15 °C to a stirred solution of Boc-β-Ala-OH (1 mmol) and NMM (0.132 ml, 1.2 mmol) in dry CH_2Cl_2 (5 ml). The temperature was maintained at −15 °C for 10 min, then (*S*)-Amp (1 mmol) and dry CH_2Cl_2 (3.6 ml) were added. The mixture was stirred at −15 °C for 15 min and then allowed to warm to room temperature. Dry DMF (10 drops) was added and stirring was continued for 1 day. Dichloromethane was added in excess and the organic layer was washed with 5% citric acid, brine, saturated aqueous $NaHCO_3$ and brine. The organic phase was dried and evaporated to give an oily residue. Purification by preparative layer chromatography [$CHCl_3$–EtOAc (3 : 1) as eluant] afforded pure **5** as an oil. Yield: 70%; $[\alpha]_D$−11°; IR ν_{max} ($CHCl_3$) 3435, 1706, 1665 cm^{-1}; ^1H NMR δ 1.14 (3H, d, $J = 6.7$ Hz $CHCH_3$), 1.46 [9H, s, $C(CH_3)_3$], 2.32–2.36 (2H, m, β-Ala α-CH_2), 2.74 and 2.83 (2H, A and B of an ABX, $J = 6.1$, 7.1 and 13.5 Hz, Amp CH_2Ph), 3.35–3.40 (2H, m, β-Ala β-CH_2), 4.30 (1H, m, Amp CH-CH_3), 5.09 (1H, br, β-Ala NH), 5.49 (1H, br, Amp NH), 7.15–7.34 (5H, m, aromatic).

X-ray diffraction. Crystals of Boc-β^3-HMet-Leu-Phe-OMe (**1a**) in the form of very tiny needles were obtained from EtOAc by slow evaporation at room temperature. X-ray data were collected at room temperature on a Rigaku AFC5R diffractometer equipped with graphite monochromatized CuKα radiation and a 12 Kw rotating anode generator. The refined cell parameters are reported in Table 1. A total of 2885 reflections ($2\theta_{max} = 124°$) were collected by the ω-2θ scan technique. Intensity data were corrected for Lorentz polarization effects and empirically for absorption. The structure was solved and refined using the program SIR 2002 [23]. Because of the few data, only the S, O and N atoms were refined anisotropically, whereas all the C atoms were refined isotropically by the full-matrix least-squares method based on 991 reflections having $I > 4\sigma(I)$. The H atoms were located at the expected positions and included in the last structure factor calculation with thermal factors deduced from the carrier atoms. The final fractional coordinates of the non-H atoms along with their thermal parameters and ESD values are available on request from the authors.

Biological Assays

Cells were obtained from the blood of healthy subjects and human peripheral blood neutrophils were purified by using the standard techniques of dextran (Pharmacia, Uppsala, Sweden) sedimentation, centrifugation on Ficoll-Paque (Pharmacia) and hypotonic lysis of contaminating red cells. Cells were washed twice and resuspended in KRPG, pH 7.4, at

Table 1 Data Collection and Refinement for Boc-β^3-HMet-Leu-Phe-OMe (**1a**)

Empirical formula	$C_{27}H_{43}N_3O_6S$
Molecular weight (a.m.u.)	537.7
Crystal system	Orthorhombic
a (Å)	21.729(3)
b (Å)	24.300(7)
c (Å)	5.982(8)
V (Å^3)	3159(4)
Space group	$P2_12_12_1$
Calculated density (g/cm^{-3})	1.131
Z	4
F(000)	1160
λ(Cu Kα) (Å)	1.5418
μ(Cu Kα) (mm^{-1})	1.2
Crystal size (mm)	$0.02 \times 0.03 \times 0.5$
$2\theta_{max}$ (°)	124
Scan type	$\omega - 2\theta$
No. unique reflections	2885
No. reflections [$I > 4\sigma(I)$]	991
Least-squares weight	$4F_o^2/\sigma^2(F_o^2)$
R,R_W	0.09, 0.12
S	0.85

a final concentration of 50×10^6 cells/ml and kept at room temperature until used. Neutrophils were 98%–100% viable, as determined using the trypan blue exclusion test.

Random locomotion. Random locomotion was performed with a 48-well microchemotaxis chamber (Bio Probe, Milan, Italy) and migration into the filter was evaluated by the leading-front method [24]. The actual random movement control was 35 ± 3 µm SE for 10 separate experiments performed in duplicate.

Chemotaxis. Each peptide was added to the lower compartment of the chemotaxis chamber. Peptides were diluted from a stock solution with KRPG containing 1 mg/ml of bovine serum albumin (Orha Behringwerke, Germany) and used at concentrations ranging from 10^{-12} to 10^{-5} M. Data were expressed in terms of chemotactic index (CI), i.e. the ratio: (migration toward test attractant minus migration toward the buffer)/migration toward the buffer. The values are the mean of six separate experiments performed in duplicate. Standard errors were in the range 0.02–0.09 CI.

Superoxide anion (O_2^-) production. This anion was measured by the superoxide dismutase-inhibitable reduction of ferricytochrome *c* (Sigma, USA) modified for microplate-based assays. Tests were carried out in a final volume of 200 µl containing 4×10^5 neutrophils, 100 nmol cytochrome *c* and KRPG. At zero time different amounts (10^{-10}–8×10^{-5} M) of each peptide were added and the plates were incubated in a microplate reader (Ceres 900, Bio-TeK Instruments) with the compartment temperature set at 37 °C. Absorbance was recorded at 550 and 468 nm. The difference in absorbance at the two wavelengths was used to calculate nmoles of O_2^- produced using an absorptivity for cytochrome c of 18.5 mM^{-1}cm^{-1}. Neutrophils were incubated with 5 µg/ml cytochalasin B (Sigma) for 5 min prior to activation by peptides. The results were expressed as net nmoles of O_2^- per 1×10^6 cells per 5 min and are the mean of six separate experiments performed in duplicate. Standard errors were in the range 0.1–4 nmole O_2^-.

Enzyme assay. The release of neutrophil granule enzymes was evaluated by determination of lysozyme activity, modified for microplate-based assays. Cells, 3×10^6/well, were first incubated in triplicate wells of microplates with 5 µg/ml cytochalasin B at 37 °C for 15 min and then in the presence of each peptide at a final concentration of 10^{-10}–8×10^{-5} M for a further 15 min. The plates were then centrifuged at $400 \times g$ for 5 min and lysozyme was quantified nephelometrically by the rate of lysis of a cell wall suspension of *Micrococcus lysodeikticus*. The reaction rate was measured using a microplate reader at 465 nm. Enzyme release was expressed as a net percentage of total enzyme content released by 0.1% Triton X-100. The total enzyme activity was 85 ± 1 µg per 1×10^7 cells/min. The values are the mean of five separate experiments performed in duplicate. Standard errors were in the range 1%–6%.

Antagonist assay. The antagonistic activity was determined by measuring the ability of a derivative to inhibit chemotaxis, superoxide anion production or granule enzyme release as induced by fMLF-OMe. Antagonistic activity data (% of activity) were obtained by comparing the chemotactic index, nmoles of O_2^- or percentage of lysozyme release in the absence (100%) and the presence of the derivative. The chemotactic index of 10 nM fMLF-OMe was 1.15 ± 0.10 SE. O_2^- generation produced by 1 µM fMLF-OMe was 62 ± 2 nmol per 1×10^6 cells per 5 min. Enzyme activity triggered by 1 µM fMLF-OMe was $54\% \pm 5\%$ per 3×10^6 cells per min. Derivatives were added to neutrophils 10 min before the incubation step for cellular

functionality. Each value represents an average of six separate experiments performed in duplicate. Standard errors were within 10% of the mean value.

RESULTS AND DISCUSSION

Biological Activity

The biological activities of the new analogues **1**–**3** were determined on human neutrophils and compared with those of the reference ligand fMLF-OMe. Directed migration (chemotaxis), superoxide anion production and lysozyme release were measured.

Inspection of Figure 2A clearly shows that all three *N*-Boc derivatives **1a**–**3a** were, as expected, essentially inactive as agonists [25]. Concerning the chemotactic activity shown by the *N*-formyl derivatives **1b**–**3b** it can be seen that the replacement of each α-amino acid residue with the corresponding β^3-amino acid led to analogues with a comparable peak of activity which was, however, lower than that shown by fMLF-OMe. Compounds **1b** and **3b**, characterized by the replacement at the two external positions, were both slightly more potent and efficient than **2b** which was characterized by the substitution at the central residue. Thus, the replacement of the central Leu, as compared with the Met and Phe residues, was the least tolerated. However, if the previously reported [5] complete inactivity of the fMLF-OMe analogue containing a central β-Ala residue is considered, the activity shown by the [β^3-HLeu^2]fMLF-OMe **2b** confirms the crucial role exerted on the activity by the central Leu hydrophobic side chain and suggests that **2b** maintains an overall accommodation in the receptor pocket comparable to that adopted by prototypical ligand and that the additional CH_2 group in the backbone does not prevent a productive, although not optimal, interaction of the central isobutyl side chain with the hydrophobic receptor subsite corresponding to the native Leu.

As shown in Figures 2B and 2C, tripeptides **1b**–**3b** were examined for the superoxide anion production and lysozyme release. It can be seen that, as already found in the case of the chemotactic activity, the less favourable modification was that performed at the central position; the [β^3-HLeu^2]fMLF-OMe analogue **2b** was indeed the least active in all experiments. On the other hand, the introduction of the β^3-residue at the *N*-terminal or at the *C*-terminal position led to highly active ligands (see **1b** and **3b** for superoxide anion and lysozyme, respectively). Since these compounds were only partially active as chemoattractants, their selective behaviour appears of interest and may represent the basis for further investigations.

All three *N*-Boc derivatives **1a**–**3a** were essentially inactive as agonists in the three tested functions (Figure 2). It seemed interesting to test their activity as antagonists. The antagonism was determined

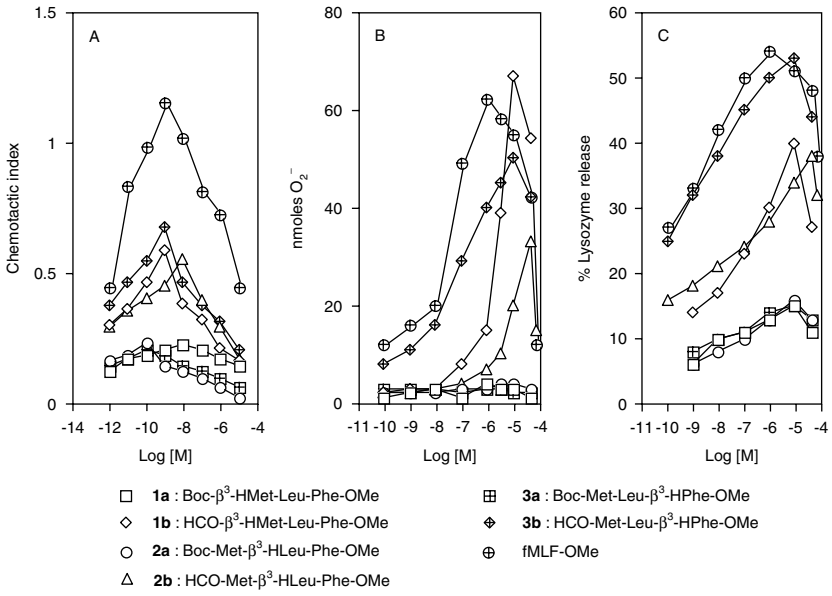

Figure 2 Biological activities of tripeptide derivatives **1a**,**b**–**3a**,**b.** (A) Chemotactic activity; (B) superoxide anion production; (C) release of neutrophil granule enzymes evaluated by determining lysozyme activity.

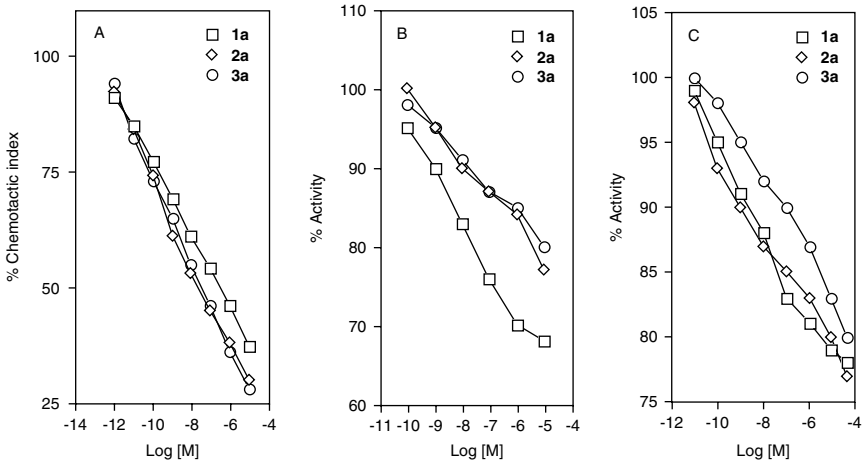

Figure 3 Effect of *N*-Boc-protected tripeptides **1a**–**3a** on the neutrophil activities triggered by fMLF-OMe. (A) Chemotactic activity; (B) superoxide anion production; (C) release of neutrophil granule enzymes evaluated by determining lysozyme activity.

by measuring the ability to inhibit the activity stimulated by fMLF-OMe on human neutrophils (Figure 3). The influence of an increasing concentration of **1a**–**3a** on chemotaxis induced by 10 nM fMLF-OMe, which is the optimal dose for chemotaxis activation, is shown in Figure 3A. A significant dose-dependent inhibition of the chemotactic index was observed for all three compounds, the inhibition becoming statistically significant ($p < 0.05$) at 10^{-10} M.

As for the superoxide anion production (Figure 3B), only the β^3-HMet analogue **1a**, the corresponding *N*-formyl analogue **1b** of which showed the highest activity as an agonist in the same test (Figure 2B), exerted a statistically significant ($p < 0.05$) inhibition on the activity induced by fMLF-OMe (starting from 10^{-7} M). In the case of the lysozyme release (Figure 3C) only a weak inhibitory action, which reached statistically significance ($p = 0.05$) only at the highest concentration, was found for the β^3-HMet[1] and β^3-HLeu[2] analogues **1a** and **2a**.

Solution Conformation

Several authors have examined the conformational preferences both in the crystal state and in solution exhibited by short linear peptides incorporating one or two β-amino acid residues [10–17]. Although the results of these investigations are difficult to summarize due to the different nature of the models examined and also the methodologies used, the overall picture clearly documents the ability of the β-residues to accommodate a wide spectrum of both folded and unfolded structures which are highly influenced by the nature of the substituents on the C^{α}–C^{β} bridge and by the constraints imposed by the neighbouring residues [26–35].

Information on the conformational preferences of the α/β^3-mixed tripeptide models studied in this work has been obtained by examining the involvement of the NH groups in intramolecular H-bonds using ^{1}H NMR. In Figure 4 the chemical shift dependence of the NH proton resonances as a function of increasing DMSO-d_6 concentrations in $CDCl_3$ solution (10 mM) is reported and in Table 2 the solvent exposure expressed as the difference ($\Delta\delta$, ppm) between the NH proton chemical shift values observed in neat $CDCl_3$ and in a $CDCl_3$ solution containing 10% DMSO. It appeared that the chemical shifts of all of three protons in each model were rather sensitive to the addition of DMSO, thus indicating the absence of high concentrations of well defined, intramolecularly H-bonded folded conformations. However, it is pertinent to note here that in all the tripeptides examined the NH group of the β^3-residue, regardless of the central or the external position occupied in the sequence, showed the lowest sensitivity to the solvent. This effect was more pronounced in the case of the two models **2b** and **3b** in which the β^3-residue was not at the *N*-terminal position.

Although the NMR titration experiments only provide an identification of potentially intramolecularly H-bonded NH groups, without giving any information on the acceptor carbonyls, the above reported behaviour of the β^3-residue NH groups suggests the occurrence, in addition to a large extent of

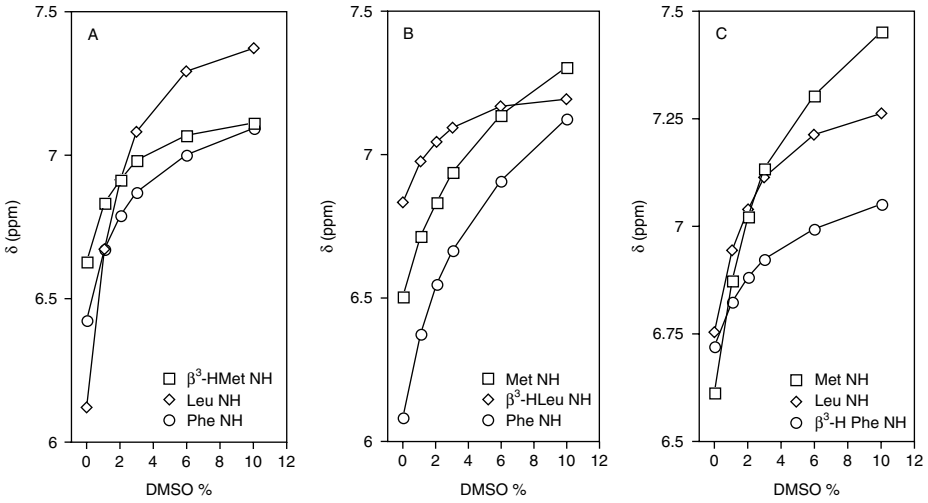

Figure 4 Plots of NH proton chemical shifts in the ^{1}H NMR spectra of *N*-formyl-tripeptides **1b** (A), **2b** (B) and **3b** (C) as a function of increasing amounts of DMSO-d_6 (v/v) added to the $CDCl_3$ solution (peptide concentration: 10 mM).

Table 2 Solvent Accessibility of Peptide NH Groups: Differences ($\Delta\delta$, ppm) between NH Proton Chemical Shift Values Observed in a $CDCl_3$ Solution Containing 10% DMSO and in Neat $CDCl_3$

Compound	*N*-Terminal NH	Central NH	*C*-Terminal NH
Boc-β^3-HMet-Leu-Phe-OMe (**1a**)	0.42	1.08	0.62
HCO-β^3-HMet-Leu-Phe-OMe (**1b**)	0.48	1.25	0.67
HCO-Met-β^3-HLeu-Phe-OMe (**2b**)	0.80	0.36	1.04
HCO-Met-Leu-β^3-HPhe-OMe (**3b**)	0.84	0.51	0.33
Boc-β-Ala-Phe-OMe (**4a**)	0.14	—	1.13
HCO-β-Ala-Phe-OMe (**4b**)	0.50	—	1.30
Boc-β-Ala-Amp (**5**)	0.19	—	1.05

unfolded conformations, of a population of locally folded conformers centred at the β-residues through a six-membered ring (C_6 conformation) [36–38]. However, the IR absorption spectra in $CHCl_3$ solution of tripeptides **1b**–**3b** did not exhibit significant absorptions in the 3400–3300 cm^{-1} region where the intramolecularly H-bonded NH groups commonly appear (spectra not shown). In the light of the recent theoretical studies on β-peptide models [37, 38], this latter finding does not appear in disagreement with the above suggested presence of C_6 local folding. Actually, calculations indicate that these small ring structures are the most stable conformers and highlight at the same time the weak stabilization produced by the intraresidue H-bond due to its unfavourable geometric parameters. Thus, this type of folding, which can be better associated with a dipole···dipole interaction, is expected to have little influence on the N-H stretching mode and the NMR chemical shift [37].

An indirect proof of the occurrence of a population of C_6 conformers in these tripeptides was obtained when the two dipeptide derivatives Boc-β-Ala-Phe-OMe (**4a**) [5] and the newly synthesized For-β-Ala-Phe-OMe (**4b**) were examined. As shown in Figure 5 and in Table 2 the β-Ala NH proton was more solvent shielded than the Phe NH proton in both compounds. Furthermore, no significant N-H stretching absorptions in the IR region below 3400 cm^{-1} were observed for these two dipeptides (spectra not shown). Also, in order to rule out the involvement of the Phe ester group as an H-bond acceptor, the model (*S*)-Boc-β-Ala-NHCH($CH_2C_6H_5$)CH_3 **(5)** was synthesized by replacing the Phe residue with Amp. Again, as shown in Table 2, the β-Ala NH proton of **5** exhibited the lowest solvent exposure. In addition,

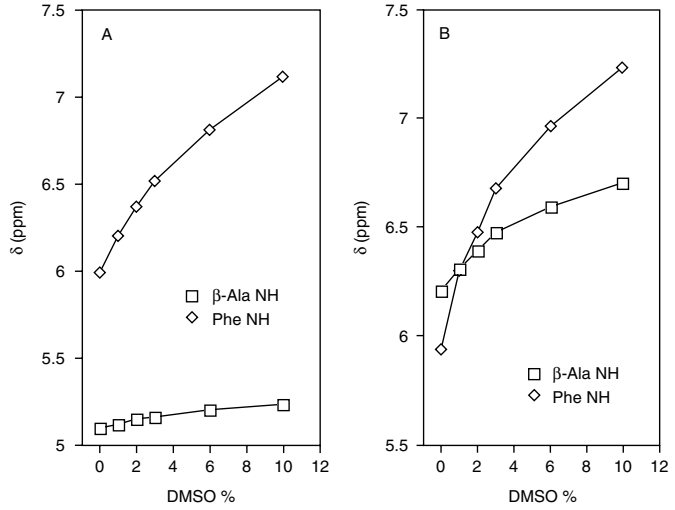

Figure 5 Plots of NH proton chemical shifts in the ^{1}H NMR spectra of dipeptide derivatives **4a** (A) and **4b** (B) as a function of increasing amounts of DMSO-d_6 (v/v) added to the $CDCl_3$ solution (peptide concentration: 10 mM).

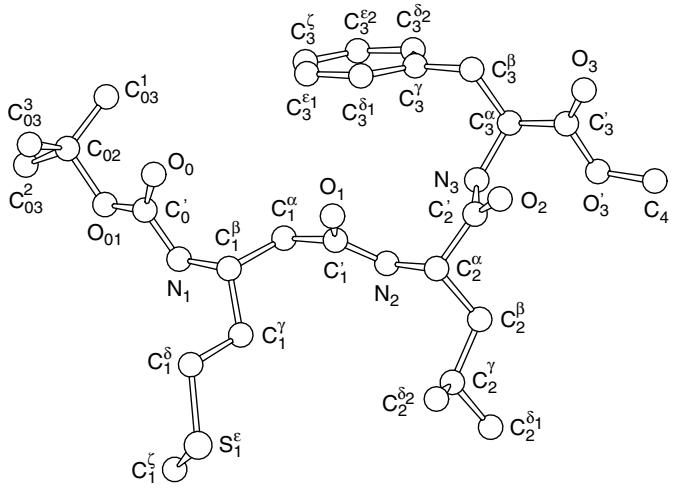

Figure 6 A perspective view of the molecular conformation found in the crystal state for the *N*-Boc-tripeptide **1a**. The numbering scheme is also shown.

no N-H stretching bands in the 3400–3300 cm^{-1} region of the IR absorption spectrum were observed (not shown).

Crystal-state Conformation of Boc-β^3-HMet-Leu-Phe-OMe (1a)

A perspective view of the molecular conformation found in the crystal of **1a**, along with the numbering scheme, is shown in Figure 6. Bond lengths and angles, although characterized by large ESD, mainly caused by the low diffracting power of the very tiny crystals obtained, are in agreement with literature values. The main torsion angles describing the crystal conformation are summarized in Table 3. The peptide backbone, described by the $\varphi_1 = -87^\circ, \theta_1 = 172^\circ, \psi_1 = 126^\circ, \varphi_2 = -86^\circ, \psi_2 = -30^\circ, \varphi_3 = 37^\circ, \psi_3 = 52^\circ$ [39], is rather extended at the β^3-HMet residue, whereas it is folded at Leu and Phe, although in the opposite screw sense. Therefore, no intramolecular H-bond is present. The two peptide bonds connecting β^3-HMet^1 to Leu^2 and Leu^2 to Phe^3 are *trans*-planar with ω values of -177° and 177°, respectively. The β^3-Met side chain adopts a partially folded conformation (g^-, t, g^-) with χ^1, χ^2 and χ^3 torsion

Table 3 Main Torsion Angles (°) Found in the Crystal State for Boc-β^3-HMet-Leu-Phe-OMe (**1a**)

C_{02}-C_{01}-C'_0-N_1	(θ_0)	−175	N_1-$C^\beta{}_1$-$C^\gamma{}_1$-$C^\delta{}_1$	($\chi_1{}^1$)	−65
O_{01}-C'_0-N_1-$C^\beta{}_1$	(ω_0)	172	$C^\beta{}_1$-$C^\gamma{}_1$-$C^\delta{}_1$-$S^\varepsilon{}_1$	($\chi_1{}^2$)	174
C'_0-N_1-$C^\beta{}_1$-$C^\alpha{}_1$	(φ_1)	−87	$C^\gamma{}_1$-$C^\delta{}_1$-$S^\varepsilon{}_1$-$C^\xi{}_1$	($\chi_1{}^3$)	−78
N_1-$C^\beta{}_1$-$C^\alpha{}_1$-C'_1	(θ_1)	172			
$C^\beta{}_1$-$C^\alpha{}_1$-C'_1-N_2	(ψ_1)	126	N_2-$C^\alpha{}_2$-$C^\beta{}_2$-$C^\gamma{}_2$	($\chi_2{}^1$)	−64
$C^\alpha{}_1$-C'_1-N_2-$C^\alpha{}_2$	(ω_1)	−177	$C^\alpha{}_2$-$C^\beta{}_2$-$C^\gamma{}_2$-$C^{\delta 1}{}_2$	($\chi_2{}^{2,1}$)	172
C'_1-N_2-$C^\alpha{}_2$-C'_2	(φ_2)	−86	$C^\alpha{}_2$-$C^\beta{}_2$-$C^\gamma{}_2$-$C^{\delta 2}{}_2$	($\chi_2{}^{2,2}$)	−63
N_2-$C^\alpha{}_2$-C'_2-N_3	(ψ_2)	−30			
$C^\alpha{}_2$-C'_2-N_3-$C^\alpha{}_3$	(ω_2)	177	N_3-$C^\alpha{}_3$-$C^\beta{}_3$-$C^\gamma{}_3$	($\chi_3{}^1$)	−55
C'_2-N_3-$C^\alpha{}_3$-C'_3	(φ_3)	37	$C^\alpha{}_3$-$C^\beta{}_3$-$C^\gamma{}_3$-$C^{\delta 1}{}_3$	($\chi_3{}^{2,1}$)	113
N_3-$C^\alpha{}_3$-C'_3-O'_3	(ψ_3)	52			
$C^\alpha{}_3$-C'_3-O'_3-C_4	(ω_3)	180			

ESD were 1°–3°.

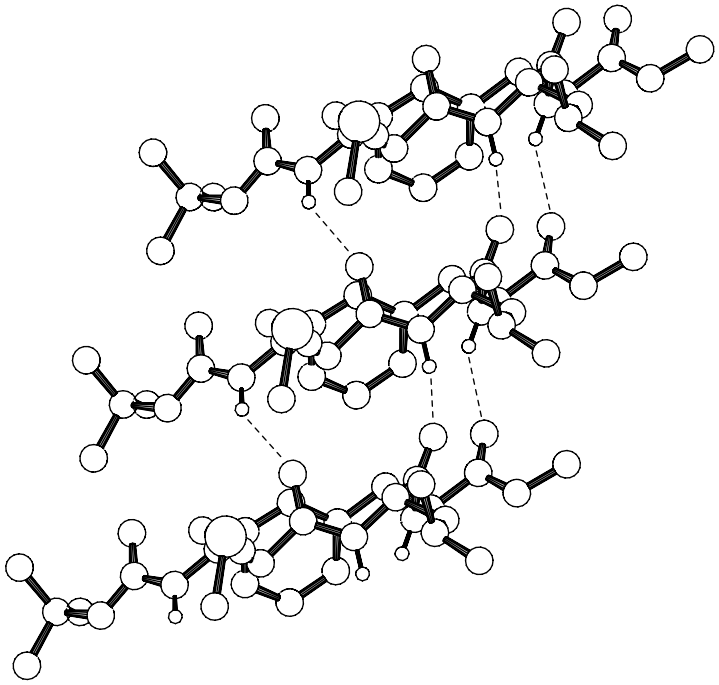

Figure 7 A view of the network of unidirectional hydrogen bonds (dashed lines) connecting molecules of **1a** in a pile elongated along the *c* direction. For clarity only the NH hydrogen atoms are shown.

angles of −65°, 174° and −78°, respectively. The Leu side chain is in the most frequently occurring $g^-(t, g^-)$ conformation, whereas the *C*-terminal Phe side chain adopts the g^- conformation ($\chi^1 = -55°$) with an orientation of the aromatic ring ($\chi^{2,1} = 113°$) slightly different from the usual value of 90° [40]. The overall peptide conformation is such that the β^3-HMet and Leu side chains lie on one side of the backbone and face each other side by side, leaving on the other side the Phe side chain, which protrudes towards the *tert*-butyl group of the Boc moiety. This spatial arrangement greatly differs from that adopted in the crystal-state by the parent fMLF-OMe [41,42], where the Leu and Phe side chains are oriented on the same side of the backbone, leaving the Met side chain on the opposite side.

An interesting aspect of the crystal-state conformation of **1a** may be found in the relative orientation of the polar NH and CO groups. As can be seen in Figure 6, all carbonyl groups point in the same

Table 4 Relevant Geometric Details of the Intermolecular H-Bonds for Compound Boc-β^3-HMet-Leu-Phe-OMe (**1a**)

Donor	Acceptor[a]	H···A (Å)	D···A (Å)	D-H···A(°)
N_1	$O^1{}_1$	2.16	2.98	143
N_2	$O^1{}_2$	1.94	2.85	157
N_3	$O^1{}_3$	2.24	3.09	147

[a] I: $x, y, z+1$
ESD 0.05–0.10 Å for distances, 1°–2° for angles.

direction that is opposite to that adopted by all the NH bonds. Moreover, the polar NH and CO groups are almost perfectly aligned along the *c* direction, thus favouring aggregation of the molecules by formation of intermolecular H-bonds along this direction. As a consequence, the crystal packing is characterized by the aggregation of piles of H-bonded molecules. Figure 7 shows the intermolecular N-H···O=C H-bonds, while Table 4 lists their relevant geometric details.

CONCLUSIONS

The results reported here give for the first time information on the consequences of the incorporation of a β^3-amino acid residue into analogues of the potent tripeptide chemoattractant fMLF-OMe. Each analogue, containing a β^3-residue and two α-residues, maintains the same side chains and stereochemistry as those present in the native ligand. Our results indicate that the α/β^3 replacements have a different and selective influence on the three biochemical functions examined here and consequently on the ability of the α/β^3 analogues to interact effectively with the appropriate receptors on the neutrophil membrane. The only common effect concerns the Leu/β^3-HLeu replacement at the central position which is in any case detrimental. Replacement of the *N*-terminal Met residue, the presence of which is critical for the activity of the fMLF analogues, leads to selective ligands: compound **1b** is in fact a modest chemoattractant but a good ligand for the superoxide anion production. Analogous considerations can be applied to the Phe/β^3-HPhe replacement at the *C*-terminal position, which affords a highly active lysozyme releaser but only a modest agonist for the other biochemical functions (compound **3b**).

As for the solution conformation adopted by the new fMLF-OMe analogues, the ^{1}H NMR titration experiments indicate, on the basis of the solvent accessibility exhibited by the NH protons that, in addition to a large amount of essentially extended conformations, a contribution of C_6 folding can be envisaged, particularly in the case of compounds **2b** and **3b**. This conclusion is in accordance with the results obtained by examining the simpler models **4** and **5** and with literature data indicating that the C_6 folding is probably only in part stabilized by H-bonding and is not easily revealed by the IR absorption spectra [37]. Thus, the ^{1}H NMR titration experiments should represent the method of choice to reveal the occurrence in solution of this elusive type of folding.

As shown in Figure 6, in the crystal-state the β^3-HMet containing model **1a** adopts a conformation which is extended at the β-residue. The torsion angles are $\varphi_1 = -87°; \theta_1 = 172°; \psi_1 = 126°$, corresponding to *skew*$^-$, *trans*$^+$ and *skew*$^+$ conformations, respectively. These values are close to those adopted in the crystal-state by one of the two independent molecules of Boc-β-Ala-Aib-OMe where the extended form coexists with the folded conformation taken up by the other molecule [31]. The conformation adopted by **1a** in the crystal-state is in accordance with the preferred conformation found in solution, where all of the three NH groups are essentially free to interact with the solvent, with the highest accessibility ($\Delta\delta = 1.08$ ppm) shown by the central Leu NH proton and the lowest ($\Delta\delta = 0.42$ ppm) by the *N*-terminal β^3-HMet NH proton. This latter value suggests that in $CDCl_3$ solution a population of C_6 folded conformer might also be present.

Acknowledgements

We are grateful to Banca del Sangue of Ferrara for providing fresh blood.

REFERENCES

1. Schiffmann E, Corcoran BA, Whal SM. N-Formylmethionyl peptides as chemoattractants for leukocytes. *Proc. Natl Acad. Sci. USA* 1975; **72**: 1059–1062.
2. Murphy PM. The molecular biology of leukocyte chemoattractant receptors. *Annu. Rev. Immunol.* 1994; **12**: 593–633.

3. Snyderman R, Uhing RJ. *Inflammation: Basic Principles and Clinical Correlates*, Gallin JI, Goldstein IM, Snyderman R (eds). Raven Press: New York, 1992; 421–439.
4. Pagani Zecchini G, Morera E, Nalli M, Paglialunga Paradisi M, Lucente G, Spisani S. Synthesis and activity on human neutrophil functions of fMLF-OMe analogs containing alkyl spacers at the central position. *Il Farmaco* 2001; **56**: 851–858.
5. Giordano C, Lucente G, Nalli M, Pagani Zecchini G, Paglialunga Paradisi M, Varani K, Spisani S. Synthesis and activity of HCO-Met-Leu-Phe-OMe analogues containing β-alanine or taurine at the central position. *Il Farmaco* 2003; **58**: 1121–1130.
6. Seebach D, Matthews JL. β-Peptides: a surprise at every turn. *Chem. Commun.* 1997; 2015–2022.
7. Gellman SH. Foldamers: a manifesto. *Acc. Chem. Res.* 1998; **31**: 173–180.
8. Gademann K, Hintermann T, Schreiber JV. β-Peptides: Twisting and turning. *Curr. Med. Chem.* 1999; **6**: 905–925.
9. De Grado WF, Schneider JP, Hamuro Y. The twists and turns of β-peptides. *J. Pept. Res.* 1999; **54**: 206–217.
10. Hill DJ, Mio MJ, Prince RB, Hughes TS, Moore JS. A field guide to foldamers. *Chem. Rev.* 2001; **101**: 3893–4011.
11. Schumann F, Muller A, Koksch M, Muller G, Sewald N. Are β-amino acids γ-turn mimetics? Exploring a new design principle for bioactive cyclopeptides. *J. Am. Chem. Soc.* 2000; **122**: 12 009–12 010.
12. Gademann K, Kimmerlin T, Hoyer D, Seebach D. Peptide folding induces high and selective affinity of a linear and small β-peptide to the human somatostatin receptor 4. *J. Med. Chem.* 2001; **44**: 2460–2468.
13. Kimmerlin T, Seebach D, Hilvert D. Synthesis of β^3-peptides and mixed α/β^3-peptides by thioligation. *Helv. Chim. Acta* 2002; **85**: 1812–1826.
14. Gopi HN, Roy RS, Raghothama SR, Karle IL, Balaram P. β-Hairpins generated from hybrid peptide sequences containing both α- and β-amino acids. *Helv. Chim. Acta* 2002; **85**: 3313–3330.
15. Sagan S, Milcent T, Ponsinet R, Convert O, Tasseau O, Chassaing G, Lavielle S, Lequin O. Structural and biological effects of a β^2- or β^3-amino acid insertion in a peptide. Application to molecular recognition of substance P by neurokinin-1 receptor. *Eur. J. Biochem.* 2003; **270**: 939–949.
16. Gung BW, Zou D, Miyahara Y. Synthesis of a hybrid peptide with both α- and β-amino acid residues: toward a new β-sheet nucleator. *Tetrahedron* 2000; **56**: 9739–9746.
17. Romanelli A, Garella I, Menchise V, Iacovino R, Saviano M, Montesarchio D, Didierjean C, Di Lello P, Rossi F, Benedetti E. Crystal-state conformation of Cα,α-dialkylated peptides containing chiral β-homoresidues. *J. Pept. Sci.* 2001; **7**: 15–26.
18. Seebach D, Abele S, Schreiber JV, Martinoni B, Nussbaum AK, Schild H, Schulz H, Hennecke H, Woessner R, Bitsch F. Biological and pharmacokinetic studies with β-peptides. *Chimia* 1998; **52**: 734–739.
19. Steer DL, Lew RA, Perlmutter P, Smith AJ, Aguilar M-I. Design and synthesis of inhibitors incorporating β-amino acids of metalloendopeptidase EC 3.4.24.15. *J. Pept. Sci.* 2000; **6**: 470–477.
20. Frackenpohl J, Arvidsson PI, Schreiber JV, Seebach, D. The outstanding biological stability of β- and γ-peptides toward proteolytic enzymes: an *in vitro* investigation with fifteen peptidases. *ChemBioChem.* 2001; **2**: 445–455.
21. Falcomer C, Vertuani G, Boggian M, Scatturin A. Formyl peptide chemoattractants. Synthesis and chemotactic activity. *Il Farmaco-Ed. Sc.* 1987; **42**: 815–822.
22. Seki M, Matsumoto K. A facile synthesis of (R)-3-amino-4-phenylbutyric acid from L-aspartic acid. *Biosci. Biotech. Biochem.* 1996; **60**: 916–917.
23. Burla MC, Camalli M, Carrozzini B, Cascarano GL, Giacovazzo C, Polidori G, Spagna R. Sir 2002: the program. *J. Appl. Crystallogr.* 2003; **36**: 1103.
24. Zigmond SH, Hirsch JG. Leukocyte locomotion and chemotaxis. New methods for evaluation and demonstration of cell-derived chemotactic factor. *J. Exp. Med.* 1973; **137**: 387–410.
25. Freer RJ, Day AR, Radding JA, Schiffmann E, Aswanikumar S, Showell HJ, Becker EL. Further studies on the structural requirements for synthetic peptide chemoattractants. *Biochemistry* 1980; **19**: 2404–2410.
26. Pavone V, Di Blasio B, Lombardi A, Isernia C, Pedone C, Benedetti E, Valle G, Crisma M, Toniolo C, Kishore R. β-Alanine and β-bends. X-ray diffraction structures of three linear oligopeptides. *J. Chem. Soc., Perkin Trans 2* 1992; 1233–1237.
27. Pavone V, Lombardi A, D'Auria G, Saviano M, Nastri F, Paolillo L, Di Blasio B, Pedone C. β-Alanine containing peptides: a novel molecular tool for the design of γ-turns. *Biopolymers* 1992; **32**: 173–183.
28. Dado GP, Gellman H. Intramolecular hydrogen bonding in derivatives of β-alanine and γ-amino butyric acid: model studies for the folding of unnatural polypeptide backbones. *J. Am. Chem. Soc.* 1994; **116**: 1054–1062.
29. Gung BW, MacKay JA, Zou D. Substituent effect on intramolecular hydrogen bonding in β-amino acid-containing polyamides. *J. Org. Chem.* 1999; **64**: 700–706.
30. Thakur AK, Kishore R. Stabilization of a novel β-turn-like motif by nonconventional intramolecular hydrogen-bonding interactions in a model peptide incorporating β-alanine. *Biopolymers* 2000; **53**: 447–454.
31. Thakur AK, Venugopalan P, Kishore R. Collateral existence of folded and extended conformations of the

β-Ala moiety in a model peptide. *Biochem. Biophys. Res. Commun.* 2000; **273**: 492–498.
32. Thakur AK, Kishore R. Influence of hydrophobic interactions on the conformational adaptability of the β-Ala residue. *J. Pept. Res.* 2001; **57**: 455–461.
33. Maji SK, Haldar D, Bhattacharyya D, Banerjee A. Conformational heterogeneity of a turn mimetic pseudo-peptide: comparison of crystal state, solution and theoretically derived structures. *J. Mol. Struct.* 2003; **646**: 111–123.
34. Günther R, Hofmann H-J. Theoretical prediction of substituent effects on the intrinsic folding properties of β-peptides. *Helv. Chim. Acta* 2002; **85**: 2149–2168.
35. Martinek TA, Fulop F. Side-chain control of β-peptide secondary structures. *Eur. J. Biochem.* 2003; **270**: 3657–3666.
36. Valle G, Bonora GM, Toniolo C. Linear oligopeptides. CV. Preferred conformations and modes of self-association of the *N-tert*-butyloxycarbonyl derivatives of glycine and β-alanine. *Gazz. Chim. Ital.* 1984; **114**: 341–347.
37. Wu Y-D, Wang D-P. Theoretical studies of β-peptides models. *J. Am. Chem. Soc.* 1998; **120**: 13 485–13 493.
38. Möhle K, Günther R, Thormann M, Sewald N, Hofmann H-J. Basic conformers in β-peptides. *Biopolymers* 1999; **50**: 167–184.
39. IUPAC-IUB Commission on Biochemical Nomenclature. Abbreviations and symbols for the description of the conformation of polypeptide chains. *J. Mol. Biol.* 1970; **52**: 1–17.
40. Benedetti E, Morelli G, Némethy G, Scheraga HA. Statistical and energetic analysis of side-chain conformations in oligopeptides. *Int. J. Pept. Protein Res.* 1983; **22**: 1–15.
41. Gavuzzo E, Mazza F, Pochetti G, Scatturin A. Crystal structure, conformation, and potential energy calculations of the chemotactic *N*-formyl-L-Met-L-Leu-L-Phe-OMe. *Int. J. Pept. Protein Res.* 1989; **34**: 409–441.
42. Jaroniec CP, Filip C, Griffin RG. 3D TEDOR NMR experiments for simultaneous measurement of multiple carbon–nitrogen distances in uniformly $^{13}C,^{15}N$-labeled solids. *J. Am. Chem. Soc.* 2002; **124**: 10 728–10 742.

